Exploring Peptide Membrane Interaction Using Surface Plasmon Resonance: Differentiation between Pore Formation versus Membrane Disruption by Lytic Peptides†

Niv Papo and Yechiel Shai*,‡

Department of Biological Chemistry, The Weizmann Institute of Science, Rehovot, 76100 Israel

Received September 3, 2002; Revised Manuscript Received November 15, 2002

ABSTRACT: Lytic peptides comprise a large group of membrane-active peptides used in the defensive and offensive systems of all organisms. Differentiating between their modes of interaction with membranes is crucial for understanding how these peptides select their target cells. Here we utilized SPR to study the interaction between lytic peptides and lipid bilayers (L1 sensor chip). Using studies also on hybrid monolayers (HPA sensor chip) revealed that SPR is a powerful tool for obtaining a real-time monitoring of the steps involved in the mode of action of membrane-active peptides, some of which previously could not be detected directly by other techniques and reported here for the first time. We investigated the mode of action of peptides that represent two major families: (i) the bee venom, melittin, as a model of a non-cell-selective peptide that forms transmembrane pores and (ii) magainin and a diastereomer of melittin (four amino acids were replaced by their D enantiomers), as models of bacteria-selective non-pore-forming peptides. Fitting the SPR data to different interaction models allows differentiating between two major steps: membrane binding and membrane insertion. Melittin binds to PC/cholesterol ∼450-fold better than its diastereomer and magainin, mainly because it is inserted into the inner leaflet (2/3 of the binding energy), whereas the other two are not. In contrast, there is only a slight difference in the binding of all the peptides to negatively charged PE/PG mono- and bilayer membranes (in the first and second steps), indicating that the inner leaflet contributes only slightly to their binding to PE/PG bilayers. Furthermore, the 100-fold stronger binding of the cell-selective peptides to PE/PG as compared with PC/cholesterol resulted only from electrostatic attraction to the negatively charged headgroups of the outer leaflet. These results clearly differentiate between the two general mechanisms: pore formation by melittin only in zwitterionic membranes and a detergent-like effect (carpet mechanism) for all the peptides in negatively charged membranes, in agreement with their biological function.

The interactions between bioactive peptides and cell membranes play a key role in many cellular processes including the action of cytolytic peptides, which comprise a large group of membrane-active peptides used in the defensive and offensive systems of all organisms. Moreover, peptides from this family serve as a nonspecific defensive system that complements the highly specific cell-mediated immune response (*1*−*6*). Interestingly, despite similarities in the structure and amino acid composition of many lytic peptides, their spectra of activities are different, and they act either on a specific or a variety of targets including bacteria, fungi, and malignant and nonmalignant cells. Numerous studies conducted on their interaction with model phospholipid membranes revealed several modes of action that can be classified into two major mechanisms: (i) the barrel-stave mechanism in which peptides insert into the hydrophobic core of the membrane and assemble therein in a barrel-stave manner to form transmembrane pores (*7*−*10*) and (ii) the carpet or the detergent-like mechanism in which peptides bind onto the surface of the membrane, predominantly by electrostatic interactions, until a threshold concentration is reached (*11*−*20*); for a recent review see ref *6*. This may eventually lead to the disruption of the membrane in a detergent-like manner. An intermediate step may include the formation of transient pores or channel aggregates, as described by the two-state or the toroidal pore formation model (*6*, *21*−*23*). Differentiating between the different mechanisms of peptide−membrane binding is crucial for understanding how these peptides select their targets. Note, for example, that the ability of a particular antimicrobial peptide to permeate model membranes does not always correlate with its biological function. This is because the peptide needs to traverse the bacterial wall (composed of lipoteichoic acid and peptidoglycan in Gram-positive and lipopolysacharides in Gram-negative bacteria) before reaching the target membrane. This step can be more difficult for one peptide than for others (*5*). For example, magainin and its cyclic form similarly bind and permeate model membranes, but only the linear form possesses high antimicrobial activity (*24*). Nevertheless, the ability of most antimicrobial peptides to permeate model phospholipid membranes is a prerequisite property for their biological function.

† This research was supported by the Israel Academy of Sciences and Humanities.

* To whom correspondence should be addressed. Tel: 972-8-9342711. Fax: 972-8-9344112. E-mail: Yechiel.Shai@weizmann.ac.il.

‡ The Harold S. and Harriet B. Brady Professorial Chair in Cancer Research.

10.1021/bi0267846 CCC: $25.00
Published on Web 12/17/2002

For the past decade, surface plasmon resonance (SPR)[1] technology, using a BIAcore biosensor, has been shown to be a powerful tool for investigating the binding behavior of macromolecules (*25*). Unlike other methods, the BIAcore technique has the combined ability to monitor the amount of adsorbed complex both continuously and with exceedingly high sensitivity, thus yielding valuable information on the kinetics and thermodynamics of the binding process. Since its commercialization, the BIAcore technique has been utilized in more than 400 studies, most of which have focused on protein−protein or protein−DNA interactions (*25*−*27*). The potential of SPR technology to provide molecular insights into biomolecular membrane interactions is not restricted only to the BIAcore instrument, as demonstrated by Vogel et al. and others (*28*−*30*). The supported lipid membrane developed by Vogel et al. was already used to evaluate the interaction between cholera toxin and the membrane-embedded receptor ganglioside G_{M1}. This system was also used to study the incorporation of the G-protein-coupled receptor rhodopsin into a membrane (*28*). Furthermore, most of these studies utilized hybrid lipid monolayers (using a HPA chip) (*31*, *32*), and only a few studies reported on the use of lipid bilayers (*33*), which constitute biological membranes. These studies include the use of a L1 sensor chip to study the interaction of the peripheral membrane protein phospholipase A_2 and its mutants with model zwitterionic and anionic membranes (*34*).

Here we used SPR spectroscopy to study the interaction between lytic peptides and both lipid monolayers (HPA sensor chip) and bilayers (L1 sensor chip) using BIAcore. To get a better understanding of the steps involved in their interaction with phospholipid membranes, we used both non-cell-selective and bacteria-selective lytic peptides that were proposed to act against the cell's membrane, via the two mechanisms described above, namely: (i) Melittin, the major component of the venom of the honey bee *Apis mellifera*, is a 26-residue amphipathic polypeptide that has non-cell-selective lytic activity (*35*) and is one of the most studied membrane-seeking polypeptides (*36*). Melittin binds strongly to both zwitterionic and negatively charged phospholipid membranes. Studies on its mode of action suggested that it forms transmembrane pores in zwitterionic lipid bilayers via a barrel-stave mechanism (*37*−*43*), but it acts as a detergent in negatively charged membranes (*44*). (ii) A synthetic diastereomer of melittin, in which four amino acids were replaced by their D enantiomers and the antimicrobial peptide magainin, which are both bacteria-selective lytic peptides that strongly bind and efficiently permeate only negatively charged membranes. Both peptides do not act via the barrel-stave mechanism but rather permeate the membrane by interacting solely with the lipidic headgroup and not with the lipidic constituent of the membrane (*45*−*48*).

Using both types of sensor chips provides real-time monitoring of the interaction of these peptides with phospholipid membranes and enables us to clearly differentiate between the two major mechanisms. Furthermore, the use of both chips enables us to distinguish between the two major steps, membrane binding and membrane insertion, and hence provides a physical explanation to the different mode of actions of closely related lytic peptides.

[1] Abbreviations: BHA, 4-methyl benzhydrylamine resin; Boc, butyloxycarbonyl; HF, hydrogen fluoride; PBS, phosphate buffered saline; PC, egg phosphatidylcholine; PE, *E. coli* phosphatidylethanolamine; PG, egg phosphatidylglycerol; Cho, cholesterol; RP-HPLC, reverse-phase high-performance liquid chromatography; SUV, small unilamellar vesicles; TFA, trifluoroacetic acid; RU, resonance signal; SPR, surface plasmon resonance.

MATERIALS AND METHODS

Materials. 4-Methyl benzhydrylamine resin (BHA) and butyloxycarbonyl (Boc) amino acids were purchased from Calibochem-Novabiochem (La Jolla, CA). Other reagents used for peptide synthesis included trifluoroacetic acid (TFA, Sigma), *N*,*N*-diisopropylethylamine (DIEA, Aldrich), methylene chloride (peptide synthesis grade, Biolab, IL), dimethylformamide (peptide synthesis grade, Biolab, IL), piperidine (Merck, Darmstadt, Germany), and benzotriazolyl-*n*-oxy-tris(dimethylamino)phosphonium-hexafluorophosphate (BOP, Sigma). Egg phosphatidylcholine (PC), egg phosphatidylglycerol (PG), phosphatidylethanolamine (PE) (Type V, from *Escherichia coli*), *N*-octyl β-D-glucopyranoside (OG), and bovine serum albumin (BSA) were purchased from Sigma. Cholesterol (extra pure) was supplied by Merck (Darmstadt, Germany). All other reagents were of analytical grade. Buffers were prepared in double glass-distilled water.

Peptide Synthesis and Purification. Native melittin and its diastereomeric analogue were synthesized by a solid-phase method on 4-methyl benzhydrylamine resin (0.05 mequiv) (*49*). Magainin was synthesized by a solid-phase method on butyloxycarbonyl-(amino acid)-(phenylacetamido) methyl resin (0.05 mmol) (*49*). All resin-bound peptides were cleaved from the resins by hydrogen fluoride (HF), and after HF evaporation and washing with dry ether, they were extracted with 50% acetonitrile/water. HF cleavage of the peptides bound to 4-methyl benzhydrylamine resin resulted in C-terminus amidated peptides. Each crude peptide contained one major peak, as revealed by RP-HPLC that was 50−70% pure by weight. The peptides were further purified by RP-HPLC on a C_{18} reverse-phase Bio-Rad semipreparative column (250 × 10 mm, 300-Å pore size, 5-μm particle size). The column was eluted in 40 min using a linear gradient of 20−80% acetonitrile in water, both containing 0.05% TFA (v/v), at a flow rate of 1.8 mL/min. The purified peptides were shown to be homogeneous (>98%) by analytical HPLC. The peptides were further subjected to amino acid analysis and electrospray mass spectroscopy to confirm their composition and molecular weight.

Preparation of Small Unilamellar Vesicles (SUV). SUVs were prepared by sonication of PC/cholesterol (10:1 w/w) or PE/PG (7:3 w/w) dispersions as previously described (*50*). Vesicles were visualized using a JEOL JEM 100B electron microscope (Japan Electron Optics Laboratory Co., Tokyo, Japan) as follows. A drop of vesicles was deposited on a carbon-coated grid and negatively stained with uranyl acetate. Examination of the grids demonstrated that the vesicles were unilamellar with an average diameter of 20−50 nm.

Binding Analysis by SPR Biosensor. Biosensor experiments were carried out with a BIAcore X analytical system (Biacore, Uppsala, Sweden) using HPA and L1 sensor chips (BIAcore). The HPA sensor chip is composed of aliphatic chains covalently bound to a gold surface. A hybrid lipid monolayer is formed when in contact with vesicles. The L1 sensor chip contains hydrophobic aliphatic chains that contain

exposed polar headgroups. Thus, when in contact with vesicles, a lipid bilayer is formed. We performed the protocol described by Aguilar et al. (*31*). Briefly, PBS (pH 6.8) was always used as the running buffer, whereas the washing solution was 40 mM *N*-octyl β-D-glucopyranoside, and the regenerating solution was 10 mM NaOH. All solutions were freshly prepared, degassed, and filtered through 0.22-μm pores. Experiments were done at 250 °C. After the BIAcore X instrument was cleaned according to the manufacturer's instruction, it was left running overnight using Milli-Q water as eluent to thoroughly wash all liquid handling parts of the instrument. The HPA (or L1) chip was then installed, and the alkanethiol surface was cleaned by an injection of the nonionic detergent, 40 mM *N*-octyl β-D-glucopyranoside (25 μL), at a flow rate of 5 μL/min. PC/cholesterol (10:1 w/w) and PE/PG (7:3 w/w) SUVs (80 μL, 0.5 mM) were then applied to the chip surface at a low flow rate (2 μL/min). To remove any multilamellar structures from the lipid surface, we injected NaOH (50 μL, 10 mM) at a flow rate of 50 μL/min, which resulted in a stable baseline corresponding to the lipid monolayer (or bilayer in the case of L1) linked to the chip surface. The negative control BSA was injected (25 μL, 0.1 mg/μL in PBS) to confirm complete coverage of the nonspecific binding sites. The monolayer (or bilayer) linked to the chip surface was then used as a model cell membrane surface to study the peptide−membrane binding.

Peptide solutions (a 30-μL PBS solution of 0.015−100 μM peptide) were injected on the lipid surface at a flow rate of 5 μL/min. PBS alone was then replaced by the peptide solution for 15 min to allow peptide dissociation. SPR detects changes in the reflective index of the surface layer of peptides and lipids in contact with the sensor chip. A sensogram was obtained by plotting the SPR angle against time. The peptide−lipid binding event was analyzed from a series of sensograms collected at seven different peptide concentrations.

Our system reached binding equilibrium during injection of the sample; therefore, the affinity constant could be calculated from the relationship between the equilibrium binding response (R_{eq} or RU_{max}) and the peptide concentration (C), using a steady-state affinity model. The affinity constants were thus determined by nonlinear least-squares (NLLSQ) fitting using the following equation:

$$RU(X) = K_A \times X \times RU_{max}/(1 + K_A \times X)$$

where X is the peptide concentration, RU_{max} is the maximal response unit (or equilibrium binding response), and K_A is the affinity constant. The affinity constant is defined as the ratio of the association and dissociation rate constants ($K_A = k_a/k_d$, with k_a and k_d having 1/M•s and 1/s units, respectively).

The sensograms for each peptide−lipid bilayer interaction (L1 chip) were also analyzed by curve-fitting using numerical integration analysis (*51*). The BIAevaluation software offers different reaction models to perform complete kinetic analyses of the peptide sensograms. One curve-fitting algorithm (the two-state reaction model) was chosen on the basis of what was known about the possible binding mechanisms of lytic peptides. The data were fit globally by simultaneously fitting the peptide sensograms obtained at seven different concentrations. The two-state reaction model was applied to each data set. This model describes two reaction steps (*31*) that, in terms of peptide−lipid interaction, correspond to

$$P + L \underset{k_{d1}}{\overset{k_{a1}}{\rightleftharpoons}} PL \underset{k_{d2}}{\overset{k_{a2}}{\rightleftharpoons}} PL^*$$

where in the first step, peptide (P) binds to lipids (L) to give PL, which is changed to PL* in the second step. PL* cannot dissociate directly to P + L and may correspond to partial insertion of the peptide into the lipid bilayer. The corresponding differential rate equations for this reaction model are represented by

$$dRU_1/dt = k_{a1} \times C_A \times (RU_{max} - RU_1 - RU_2) - k_{d1} \times RU_1 - k_{a2} \times RU_1 + k_{d2} \times RU_2$$

$$dRU_2/dt = k_{a2} \times RU_1 - k_{d2} \times RU_2$$

where RU_1 and RU_2 are the response units for the first and second steps, respectively, C_A is the peptide concentration, RU_{max} is the maximal response unit (or equilibrium binding response), and k_{a1}, k_{d1}, k_{a2}, and k_{d2} are the association and dissociation rate constants for the first and second steps, respectively. k_{a1} has 1/(M•s) units, and k_{d1}, k_{a2}, and k_{a2} have 1/s units. Thus, the total affinity constant for all processes, K, has M^{-1} units.

RESULTS

We utilized a BIAcore biosensor method to investigate the mode of action of lytic peptides that represent two major families: (i) Melittin, as a model for a non-cell-selective lytic peptide that forms transmembrane pores in zwitterionic phospholipid membranes presumably via the barrel-stave mechanism and acts in a detergent-like manner on negatively charged membranes. (ii) Magainin and a diastereomer of melittin, as models for nonhemolytic antimicrobial peptides that permeate preferentially negatively charged membranes by interacting with the acidic phospholipid headgroups via the carpet mechanism. The sequences of the peptides are shown in Table 1.

Binding Affinity of the Peptides to Lipid Monolayers and Bilayers Measured by SPR.

Steady-State Affinity Model for Peptide Binding to Membranes. PC/cholesterol (10:1 w/w) and PE/PG (7:3 w/w) monolayers and bilayers were absorbed onto the HPA and L1 chips, respectively. Typical sensograms of the binding between magainin, melittin diastereomer, and melittin with bilayers of PC/cholesterol (10:1 w/w) and PE/PG (7:3 w/w) are shown in Figures 1−3, panels A and B. The sensograms of the binding between melittin with lipid monolayers showed markedly lower response levels as compared with their binding to bilayers (four and two times lower in the case of PC/cholesterol and PE/PG, respectively, figure not shown). However, the sensograms of the binding between magainin and the melittin diastereomer with lipid monolayers showed similar response levels as compared to their binding to bilayers (figure not shown). These results indicate that whereas the membrane's inner layer increases the binding of melittin to the lipid bilayer, it has no influence on the interaction of magainin and the melittin diastereomer with lipid bilayers. Note also that although all the peptides

Table 1: Designations, Sequences, and Retention Times of the Peptides Investigated

peptide designation	sequence[a]	RP-HPLC retention time (min)[b]
non-pore-forming peptides		
magainin	GIGKFLHSAKKFGKAFVGEIMNS-COOH	17.03
melittin diastereomer	GIGA**V**LK**V**LTTGLPAL**I**SWI**K**RKRQQ-NH_2	18.41
pore-forming peptide		
melittin	GIGAVLKVLTTGLPALISWIKRKRQQ-NH_2	24.95

[a] Underlined and bold amino acids are D enantiomers. [b] A C_{18} reverse-phase analytical column was used. The peptides were eluted in 40 min, using a linear gradient of 20−80% acetonitrile in water, both containing 0.05% TFA (v/v).

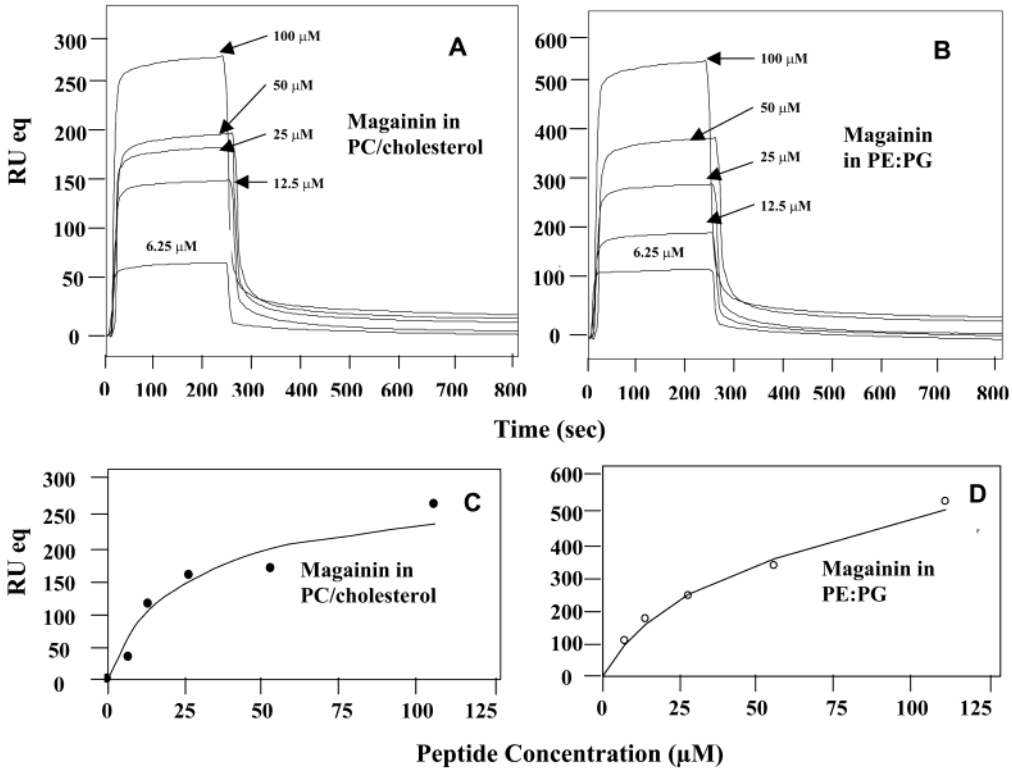

FIGURE 1: Panels A and B: Sensograms of the binding between various concentrations of magainin and the lipid bilayer (L1 chip), PC/cholesterol (10:1 w/w) (panel A), and PE/PG (7:3 w/w) (panel B). Panels C and D: The corresponding relationships between the equilibrium binding response (RU_{eq}) and the peptide concentration (*C*) (circles). The data were fit using the BIAcore's steady-state affinity model (lines). Magainin concentrations used are 6.25, 12.5, 25, 50, and 100 μM.

reached similar levels when bound to PC/cholesterol bilayers (Figures 1−3, panel A), melittin concentrations (0.015, 0.03, 0.07, 0.15, and 0.3 μM) were much lower than those of magainin and the melittin diastereomer (6.25, 12.5, 25, 50, and 100 μM), demonstrating the higher affinity of melittin toward PC/cholesterol bilayers.

The sensograms revealed that the RU signal intensity increased as a function of the peptide's concentration. This indicates that the amount of peptide bound to the lipids is proportional to the increase in peptide concentration. On the other hand, the data show that the curves of melittin obtained by using acidic bilayers (Figure 3B) or zwitterionic bilayers (Figure 3A) reached similar levels. On the other hand, similar concentrations of magainin and the melittin diastereomer gave higher levels (two times higher) in the binding sensograms of acidic bilayers (Figures 1B and 2B, respectively) as compared with zwitterionic bilayers (Figures 1A and 2A, respectively). Similar results were obtained by using monolayers instead of bilayers (figure not shown). These results correlate with the nonselective activity of melittin toward zwittereionic and negatively charged membranes as compared with the selective activity of magainin and the melittin diastereomer to negatively charged phospholipids.

Our system reached binding equilibrium during the injection of the sample; therefore, the affinity constants could be calculated from the relationship between the equilibrium binding response (R_{eq}) and the peptide's concentration (*C*), using a steady-state affinity model (Figures 1−3, panels C and D). The affinity constants are defined as the ratio of the association and dissociation rate constants ($K_A = k_a/k_d$). Table 2 shows the affinity constants of the peptides to both zwitterionic and negatively charged membranes, as well as the ratio between the affinity constants to bilayers and monolayers. The data reveal that the affinity of the antimicrobial peptides magainin and the melittin diastereomer to negatively charged phospholipid membranes is ∼100-fold higher than to zwitterionic membranes, similar to what has been obtained by other methods (*47*, *52*). This indicates that electrostatic interactions play an important role in their affinity to membranes. In contrast, the affinity of melittin to monolayers is not affected by the charge of the phospholipid headgroup and is only slightly higher in zwitterionic than

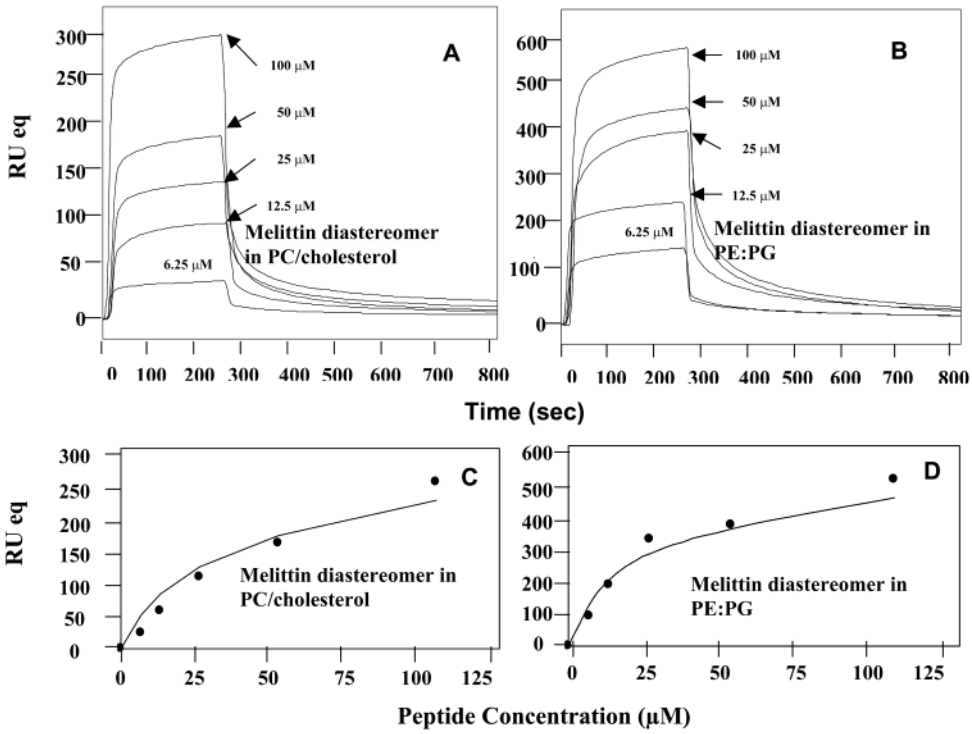

FIGURE 2: Panels A and B: Sensograms of the binding between various concentrations of the melittin diastereomer and the lipid bilayer (L1 chip), PC/cholesterol (10:1 w/w) (panel A), and PE/PG (7:3 w/w) (panel B). Panels C and D: The corresponding relationships between the equilibrium binding response (RU_{eq}) and the peptide concentration (*C*) (circles). The data were fit using the BIAcore's steady-state affinity model (lines). Peptide concentrations used are 6.25, 12.5, 25, 50, and 100 μM.

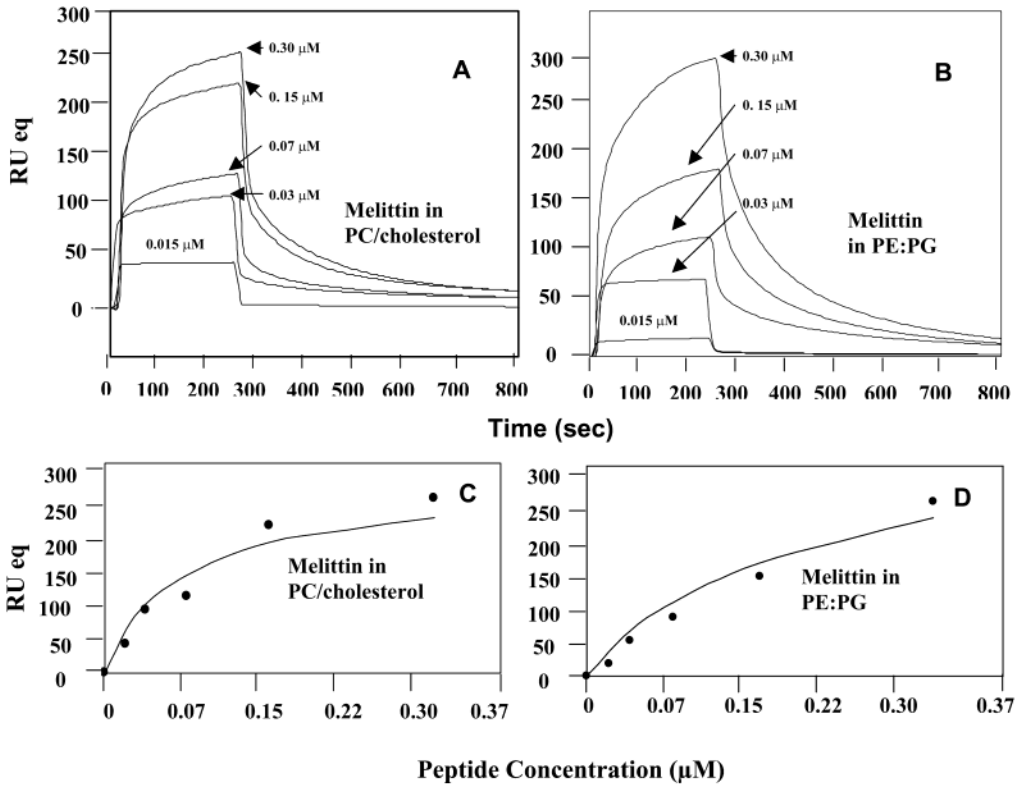

FIGURE 3: Panels A and B: Sensograms of the binding between various concentrations of melittin and the lipid bilayer (L1 chip), PC/cholesterol (10:1 w/w) (panel A), and PE/PG (7:3 w/w) (panel B). Panels C and D: The corresponding relationships between the equilibrium binding response (RU_{eq}) and the peptide concentration (*C*) (circles). The data were fit using the BIAcore's steady-state affinity model (lines). Melittin concentrations used are 0.015, 0.03, 0.07, 0.15, and 0.3 μM.

negatively charged phospholipid bilayers. This indicates that the affinity of melittin to membranes is driven predominantly by hydrophobic interactions.

The difference between the affinity of the peptides to monolayers as compared to bilayers should indicate the contribution of the inner leaflet to the binding process. The

Table 2: Equilibrium Affinity Constants of the Peptides with PC/Cholesterol and PE/PG Monolayers (HPA Chip) and Bilayers (L1 Chip) Derived According to a Steady-State Affinity Model

	PC/Cholesterol (10:1 w/w)			PE/PG (7:3 w/w)		
	K_A ($\times 10^4$ M^{-1})			K_A ($\times 10^4$ M^{-1})		
peptide designation	monolayer	bilayer	$K_{A\ bilayer}/K_{A\ monolayer}$	monolayer	bilayer	$K_{A\ bilayer}/K_{A\ monolayer}$
magainin	0.11 (±0.01)	0.09 (±0.01)	0.80	3.23 (±0.12)	10.9 (±0.8)	3.4
melittin diastereomer	0.13 (±0.01)	0.11 (±0.01)	0.85	3.70 (±0.15)	12.9 (±0.9)	3.5
melittin	1.88 (±0.09)	47 (±3)	25	1.89 (±0.02)	15.9 (±0.9)	8.4

Table 3: Association (k_{a1}, k_{a2}) and Dissociation (k_{d1}, k_{d2}) Rate Constants in Bilayers Determined by Numerical Integration Using the Two-State Reaction Model[a]

peptides	lipid	k_{a1} (1/M·s)	k_{d1} (1/s)	K_1 ($\times 10^4$ 1/M)	k_{a2} (1/s)	k_{d2} (1/s)	K_2	K ($\times 10^4$ 1/M)
magainin	PC/cholesterol	1.9 (±0.1)	0.0070 (±0.0006)	0.03	0.041 (±0.003)	0.0090 (±0.0004)	4.5	0.12 (±0.01)
	PE/PG	19.6 (±0.9)	0.0007 (±0.0001)	2.8	0.059 (±0.004)	0.018 (±0.002)	3.3	9.2 (±0.9)
melittin diastereomer	PC/cholesterol	2.1 (±0.1)	0.0080 (±0.0006)	0.03	0.062 (±0.005)	0.020 (±0.002)	3.1	0.081 (±0.007)
	PE/PG	18.8 (±0.8)	0.00060 (±0.00003)	3.1	0.049 (±0.004)	0.015 (±0.001)	3.3	10.2 (±0.1)
melittin	PC/cholesterol	19.0 (±1.5)	0.00050 (±0.00004)	3.8	0.410 (±0.04)	0.025 (±0.002)	16.5	62.3 (±3.4)
	PE/PG	15.5 (±1.1)	0.00040 (±0.00003)	3.9	0.115 (±0.01)	0.016 (±0.001)	7.2	27.9 (±1.7)

[a] The affinity constants K_1 and K_2 are for the first ($K_1 = k_{a1}/k_{d1}$) and second ($K_2 = k_{a2}/k_{d2}$) steps, respectively, and the affinity constant (K) determined as $(k_{a1}/k_{d1}) \times (k_{a2}/k_{d2})$ is for the complete binding process.

values of the ratio $K_{A\ bilayers}/K_{A\ monolayer}$, listed in Table 2, demonstrate that the binding of magainin, as well as the melittin diastereomer to PC/cholesterol monolayers, is similar to their binding to bilayers, indicating that the peptides are not influenced by the membrane's inner layer. Thus, these two peptides do not insert into the PC/cholesterol bilayers. However, their binding to PE/PG bilayers is slightly higher than to monolayers (~3.5-fold higher, Table 2), indicating that they are slightly influenced by the inner layer and thus are partially inserted into the inner leaflet of PE/PG bilayers. This process might relate to the translocation of magainin into the inner leaflet (*52*). A different situation is observed with melittin. Its affinity to PC/cholesterol bilayers is 25-fold higher than to monolayers, indicating that melittin is inserted deeply into the inner membrane. Since melittin's interaction with PC/cholesterol membranes is driven predominantly by hydrophobic interaction, these results support the pore-forming property of melittin as proposed by others (*36*−*42*). As compared to PC/cholesterol membranes, the affinity of melittin to PE/PG bilayers is only ~8.5-fold higher than to monolayers, indicating a mechanism that includes predominatly a detergent-like effect as proposed by others (*44*).

Two-State Model for the Peptide's Binding to Membranes. We employed numerical integration analysis that uses nonlinear analysis to fit an integrated rate equation directly to the sensograms (*31*). When fitting the peptide's sensograms globally (using different concentrations of the peptides) with the simplest 1:1 Langmuir binding model, a poor fit was obtained (data not shown), confirming that this model does not represent the lipid binding mechanism of all the peptides investigated. However, a significantly improved fit was obtained using numerical integration of the two-state reaction model of the binding sensograms. This model reflects a two-step process in the interaction of the peptides with lipid bilayers: the first step is the actual binding, and the second step is the insertion of the peptide into the membrane. A set of peptide sensograms with seven different peptide concentrations was used to estimate the kinetic parameters. The average values for the rate constants obtained from the two-state model analysis are listed in Table 3 along with the affinity constant values (K). The data are shown only for peptide−bilayer interactions (L1 sensor chip). The data reveal several important observations. First, the affinity constants, K, determined by using the two-state model are similar to those obtained by directly fitting the data using a steady-state model (see previous paragraph and Table 2). Second, the higher affinity of the antimicrobial peptides magainin and the melittin diastereomer to PE/PG as compared with PC/cholesterol membranes is the result of the first step and not the second step. This is because they bind ~10-fold faster (k_{a1}) and dissociate ~10-fold slower (k_{d1}) from PE/PG than PC/cholesterol in the first step, but they have similar binding rate constants in PE/PG and in PC/cholesterol in the second step (Table 3). Third, whereas melittin dissociates in the second step similarly to the other two peptides in both PE/PG and PC/cholesterol, its association with PE/PG and PC/cholesterol is ~ 2−3-fold and ~8−10-fold, respectively, faster than the other two peptides. This indicates that the major difference between melittin and the other two peptides is in the insertion process. Interestingly, however, melittin binds and dissociates with similar rates from both PC/cholesterol and PE/PG membranes only in the first step. These results indicate a major difference between the mode of action of melittin and the other two peptides in PC/cholesterol and to a lesser extent into PE/PG membranes. In other words, melittin inserts into the inner membrane of PC/cholesterol but to a lesser extent to PE/PG membranes. Note that in all cases, the second step (K_2, insertion) was slower than the first (K_1, initial binding). The experiments were repeated three times with a standard deviation of 10%.

DISCUSSION

The present study demonstrates that SPR is a powerful tool for investigating real-time interactions between membrane-active peptide and lipid monolayers and bilayers, and as a result, allows distinguishing between different modes of action. This is because it allows continuous monitoring of

two major steps: first, the peptide's association with the membrane, followed by a second slower process of insertion into the hydrophobic core or into the inner surface of the bilayer. We used liposomes, mimicking the outer leaflet plasma membrane of bacteria and erythrocytes, as well as native and synthetic peptides with different modes of action; melittin, which forms pores in zwitterionic membranes via the barrel stave mechanism, and magainin and a diastereomer of melittin, which do not form transmembrane pores.

Selection of the Target Membrane Takes Place in the First Step. The data show a marked difference between melittin and the two antimicrobial peptides magainin and the melittin diastereomer. Importantly, all the parameters determined for magainin and the melittin diastereomer are identical (Tables 2 and 3, within the error of the measurements), suggesting that both act via a similar mechanism, in agreement with their nonhemolytic and antimicrobial activity (*45*−*47*). Similarly to what has been shown by other methods, magainin and the melittin diastereomer interact preferentially with anionic lipids ∼100-fold stronger than that with zwitterionic lipids (Tables 2 and 3). The BIAcore studies show that this difference in binding is mainly due to the first binding step. Furthermore, this preferential binding is due to both an increase of ∼10-fold in the rate of association (k_{a1}, Table 3) and a decrease of ∼10-fold in the rate of dissociation (k_{d1}, Table 3) from PE/PG as compared with PC/cholesterol. Thus, the first step is mainly governed by electrostatic interactions between the peptide and the membrane. In contrast, in the second step, the rates of association (k_{a2}, Table 3) and dissociation (k_{d1}, Table 3) are similar for both PE/PG and PC/cholesterol, indicating that electrostatic interactions are not important for the insertion of the peptides into the membrane. The difference between the binding constants measured by using SPR (the present study) and the tryptophan fluorescence experiments reported elsewhere (*47*) is the result of the difference in the methods and the experimental conditions used. More specifically: (i) the detection of membrane binding by using tryptophan fluorescence can be done only when the fluorescence of tryptophan is significantly changed upon membrane binding. However, if tryptophan does not move to a detectable hydrophobic environment such as on the surface of the membrane and with an affinity less than 10^3 (as in the case of the diastereomer of melittin in Oren and Shai (*47*)), it would be difficult to detect membrane binding. (ii) The phospholipids used in Oren and Shai (*47*) are different from those used in the present study. (iii) Tryptophan fluorescence experiments measure a peptide's binding to vesicles under steady-state conditions (i.e., the maximum bound peptide after equilibrium is reached). However, the SPR technique calculates the binding constant in real-time during the whole binding process and at different peptide concentrations, which should be more accurate. Ladokin and White (*48*) used the equilibrium dialysis method and also could detect binding of the diasteromer of melittin to PC alone (with no cholesterol) with a partition constant that is ∼10-fold weaker than in this study.

As compared with the two antimicrobial peptides, melittin binds strongly to both types of lipids. Note that the binding constant of melittin and magainin to the negatively charged lipids PE/PG that we used is about 10−100-fold weaker than that reported by others using PC/PG or DMPG instead (*31*, *38*). In addition, the peptides' affinity to PC/cholesterol is 2−9-fold weaker than that reported by Mozsolits et al. (*31*). When we substituted PE for PC or used only PG, we detected an increase in the binding constant by more than 10-fold. Furthermore, when we substituted PC/cholesterol for PC, we observed a 2−10-fold increase in the binding constant (data not shown). Note also that melittin binds similarly to monolayers composed of PC/cholesterol and PE/PG, but its binding to PC/cholesterol is slightly increased as compared to PE/PG when bound to bilayers (Table 2). The rate constants shown in Table 3 reveal that this difference is mainly due to the insertion process in step 2. Moreover, Table 3 shows that k_{a1} is the same for PC/cholesterol and PE/PG, but k_{a2} is about 3-fold higher for PC/cholesterol than to PE/PG. A plausible explanation is the tighter association of the positively charged melittin with the negatively charged surface of PE/PG as compared to a zwitterionic surface of PC/cholesterol, which makes it more difficult for melittin to insert into the hydrophobic core. The weaker ability of melittin to insert into PE/PG as compared with PC/cholesterol supports the notion that melittin acts, at least partially, in a detergent-like manner when it binds to negatively charged membranes (*44*).

The rate constants of the second step further support the assumption that melittin forms stable pores in PC/cholesterol membranes. Note that whereas the ratio between the rate of association and dissociation is 3−4.5 for the antimicrobial peptides magainin and the melittin diastereomer, the ratio is 16.5 for melittin.

Binding to Monolayers versus Bilayers. The advantage of comparing both monolayers and bilayers is that it allows examining directly the effect of the membrane's inner layer with regard to the binding properties of the peptides. Table 2 shows that there is no difference between the affinity of the antimicrobial peptides magainin and the melittin diastereomer to PC/cholesterol monolayers as compared to bilayers. This indicates that the inner membrane does not participate in the binding, or in other words, the antimicrobial peptides do not insert into the inner PC/cholesterol membrane. In contrast, there was a 25-fold increase in the binding of melittin to PC/cholesterol bilayers as compared with monolayers. This strongly suggests that melittin inserts into the hydrophobic core of the membrane (Figure 4D). Furthermore, the finding that the binding constant, K_1, in the two-step model (Table 3) is very similar to the binding constant for the monolayer, K_A (Table 2), also supports the notion that the increase in binding results from the insertion of melittin in the second step. However, a different situation was observed with PE/PG membranes. Table 2 shows only ∼3.5-fold increase in the binding of magainin and the melittin diastereomer to bilayers as compared with monolayers. This supports the notion that the inner bilayer is weakly involved in the binding process. This is also confirmed by the finding that the binding constants for both peptides, K_1, in the first step of the two-step model (Table 3) are very similar ($\sim 3 \times 10^4\ M^{-1}$) to the binding constant for the monolayer, K_A (Table 2). This is in line with the partial translocation of magainin into the inner membrane, probably through intermediate transient pores (Figure 4, panel C), but this does not support a trans membrane pore formation mechanism similar to melittin. Interestingly, there is an 8.4-fold increase in the binding of melittin to PE/PG

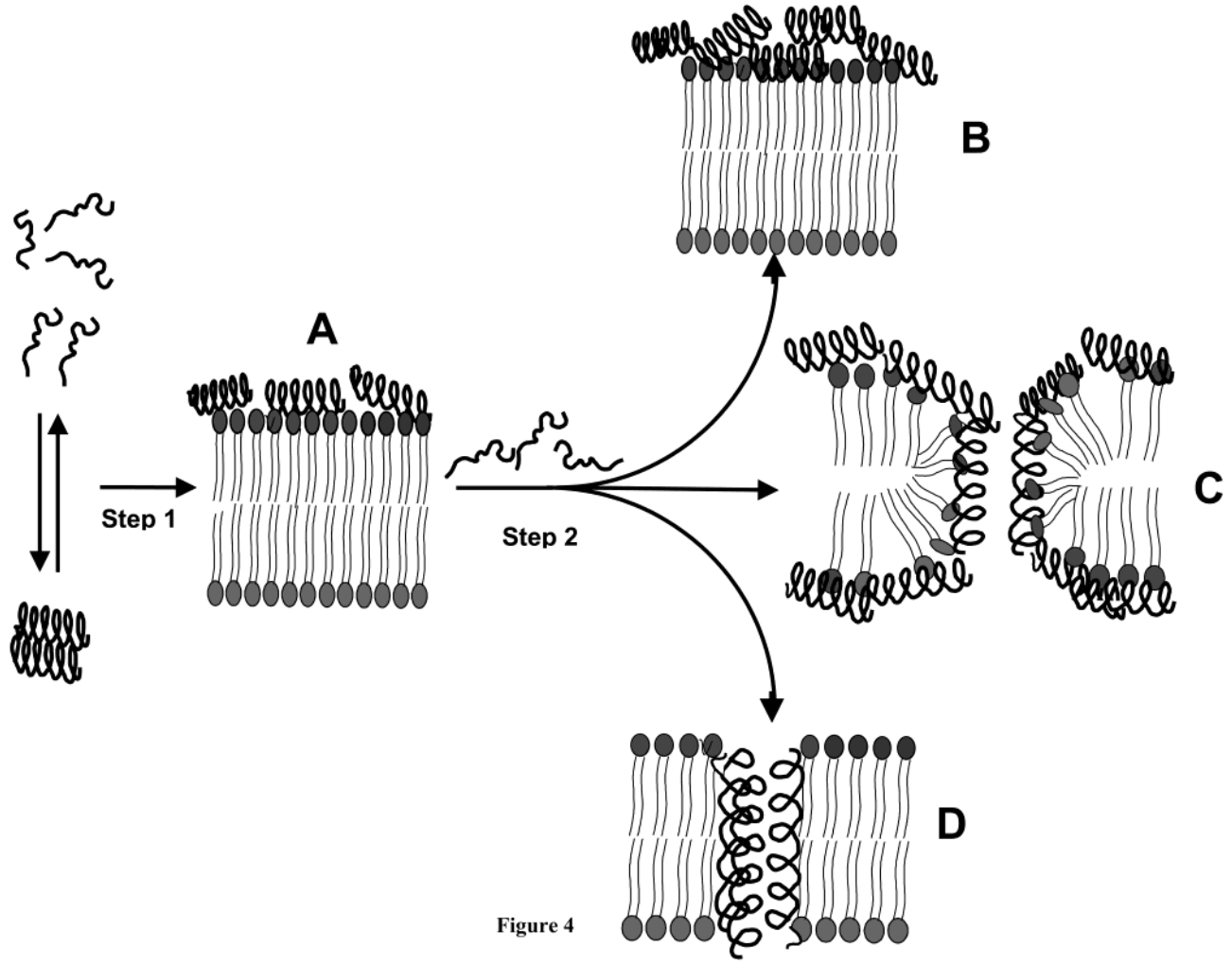

FIGURE 4: Schematic representation of the different mechanisms of membrane lysis by the peptides. Peptides bind in the first step mainly by electrostatic interactions and align parallel to the outer membrane surface (A). Increasing peptide concentration does not affect the interaction of magainin and the melittin diastereomer with PC/cholesterol (B). In contrast, increasing the concentration of magainin and the melittin diastereomer causes initial permeation of PE/PG membranes (C) followed by membrane disintegration. The peptides remain in contact with the headgroup region of the lipid bilayer during the whole process, as described in the carpet model (*58*, *59*). Finally, melittin inserts deeply into the hydrocarbon region of PC/cholesterol membranes (D) and forms transmembrane pores by the assembly of several monomers via a barrel-stave mechanism (*7*).

bilayers as compared with monolayers. This value is less than that found for melittin in PC/cholesterol but higher than that found for magainin and the melittin diastereomer in PE/PG. This strengthens the evidence for a situation in which melittin acts, at least partially, as a detergent in negatively charged membranes.

Our BIAcore studies are in agreement with other studies on the mode of action of melittin in zwitterionic and negatively charged membranes. It has been shown that melittin forms pores in POPC vesicles (*43*, *53*), but it causes a detergent-like release from POPG vesicles (*44*). Furthermore, oriented circular dichroism experiments with melittin in oriented POPC and POPG multibilayers showed that melittin can adopt a transmembrane configuration only in POPC multilayers (*54*). It has been proposed that melittin cannot insert and readily adopt a transmembrane orientation in anionic bilayers because of an increased kinetic barrier because of strong electrostatic interactions of melittin with the negatively charged lipids, or alternatively, because a new type of pore with helices parallel to the membrane plane is being formed (*44*). Aggregation of such surface-bound helices might induce and enhance the effect on the local bilayer thickness. The detergent-like action may therefore occur because surface-bound melittin aggregates reduce bilayer thickness and consequently cause local structural instabilities and fluctuations equivalent to transient pores. Such structures were also described as transient pores in toroidal pore formation and the carpet mechanism (Figure 4B).

The finding that the binding of magainin and the melittin diastereomer to PC is similar in mono- and bilayers suggests that they do not interact with the hydrophobic core of the membrane, and thus, stay localized on the membrane surface (Figure 4A). Therefore, the increase in their binding to PE/PG bilayers as compared with monolayers indicates that that they translocate into the inner membrane by interacting with the headgroup, as proposed by Matsuzaki and co-workers (*52*), and by the carpet mechanism (*55*). The inability of the melittin diastereomer and magainin to insert into the hydrophobic core of the membrane as compared to melittin is also supported by FTIR studies, which showed that magainin and the melittin diastereomer did not change the lipid order of PC and PE/PG, whereas melittin did (*47*, *56*, *57*).

In summary, we have shown that SPR is a fast and powerful tool to obtain real-time monitoring of the steps governing the mode of action of membrane-active peptides, some of which could not be detected directly by other means. The binding constants obtained herein using the BIAcore biosensor are similar to those values obtained by using different techniques such as equilibrium dialysis (*48*) and tryptophan fluorescence (*38*, *47*). However, the SPR studies clearly differentiate between the two steps involved in membrane binding and permeation via the two general mechanisms, namely, pore formation by melittin only in zwitterionic membranes and a detergent-like effect (a carpet mechanism) for all the peptides in negatively charged membranes, which is in agreement with their biological function. Similar studies should assist in the rapid screening of antimicrobial peptides urgently needed because of the increasing resistance of harmful microorganisms to the available antibiotics.

REFERENCES

1. Boman, H. G. (1995) *Annu. Rev. Immun. 13*, 61−92.
2. Nicolas, P., and Mor, A. (1995) *Annu. Rev. Microbiol. 49*, 277−304.
3. Lehrer, R. I., and Ganz, T. (1999) *Curr. Opin. Immunol. 11*, 23−27.
4. Hoffmann, J. A., Kafatos, F. C., Janeway, C. A., and Ezekowitz, R. A. (1999) *Science 284*, 1313−1318.
5. Hancock, R. E., and Diamond, G. (2000) *Trends Microbiol. 8*, 402−410.
6. Zasloff, M. (2002) *Nature 415*, 389−395.
7. Ehrenstein, G., and Lecar, H. (1977) *Q. Rev. Biophys. 10*, 1−34.
8. Rizzo, V., Stankowski, S., and Schwarz, G. (1987) *Biochemistry 26*, 2751−2759.
9. Shai, Y., Bach, D., and Yanovsky, A. (1990) *J. Biol. Chem. 265*, 20202−20209.
10. Rapaport, D., and Shai, Y. (1991) *J. Biol. Chem. 266*, 23769−23775.
11. Pouny, Y., Rapaport, D., Mor, A., Nicolas, P., and Shai, Y. (1992) *Biochemistry 31*, 12416−12423.
12. Gazit, E., Boman, A., Boman, H. G., and Shai, Y. (1995) *Biochemistry 34*, 11479−11488.
13. Strahilevitz, J., Mor, A., Nicolas, P., and Shai, Y. (1994) *Biochemistry 33*, 10951−10960.
14. La Rocca, P., Biggin, P. C., Tieleman, D. P., and Sansom, M. S. (1999) *Biochim. Biophys. Acta 1462*, 185−200.
15. Oren, Z., Lerman, J. C., Gudmundsson, G. H., Agerberth, B., and Shai, Y. (1999) *Biochem. J. 341*, 501−513.
16. Wong, H., Bowie, J. H., and Carver, J. A. (1997) *Eur. J. Biochem. 247*, 545−557.
17. Monaco, V., Formaggio, F., Crisma, M., Toniolo, C., Hanson, P., and Millhauser, G. L. (1999) *Biopolymers 50*, 239−253.
18. Fernandez-Lopez, S., Kim, H. S., Choi, E. C., Delgado, M., Granja, J. R., Khasanov, A., Kraehenbuehl, K., Long, G., Weinberger, D. A., Wilcoxen, K. M., and Ghadiri, M. R. (2001) *Nature 412*, 452−455.
19. Mattute, B., Knoop, F. C., and Conlon, J. M. (2000) *Biochem. Biophys. Res. Commun. 268*, 433−436.
20. Whiles, J. A., Brasseur, R., Glover, K. J., Melacini, G., Komives, E. A., and Vold, R. R. (2001) *Biophys. J. 80*, 280−293.
21. Ludtke, S. J., He, K., Heller, W. T., Harroun, T. A., Yang, L., and Huang, H. W. (1996) *Biochemistry 35*, 13723−13728.
22. Matsuzaki, K. (1999) *Biochim. Biophys. Acta 1462*, 1−10.
23. Hancock, R. E., and Rozek, A. (2002) *FEMS Microbiol. Lett. 206*, 143−149.
24. Oren, Z., and Shai, Y. (2000) *Biochemistry 39*, 6103−6114.
25. Hall, D. (2001) *Anal. Biochem. 288*, 109−125.
26. Carrick, F. E., Forbes, B. E., and Wallace, J. C. (2001) *J. Biol. Chem. 276*, 27120−27128.
27. Nguyen, B., Tardy, C., Bailly, C., Colson, P., Houssier, C., Kumar, A., Boykin, D. W., and Wilson, W. D. (2002) *Biopolymers 63*, 281−297.
28. Heyse, S., Ernst, O. P., Dienes, Z., Hofmann, K. P., and Vogel, H. (1998) *Biochemistry 37*, 507−522.
29. Salamon, Z., Meyer, T. E., and Tollin, G. (1995) *Biophys. J. 68*, 648−654.
30. Salamon, Z., Wang, Y., Soulages, J. L., Brown, M. F., and Tollin, G. (1996) *Biophys. J. 71*, 283−294.
31. Mozsolits, H., Wirth, H. J., Werkmeister, J., and Aguilar, M. I. (2001) *Biochim. Biophys. Acta 1512*, 64−76.
32. Wang, W., Smith, D. K., Moulding, K., and Chen, H. M. (1998) *J. Biol. Chem. 273*, 27438−27448.
33. Mozsolits, H., and Aguilar, M. I. (2002) *Biopolymers 66*, 3−18.
34. Stahelin, R. V., and Cho, W. (2001) *Biochemistry 40*, 4672−4678.
35. Habermann, E., and Jentsch, J. (1967) *Hoppe-Seyler's Z. Physiol. Chem. 348*, 37−50.
36. Dempsey, C. E. (1990) *Biochim. Biophys. Acta 1031*, 143−161.
37. Vogel, H., and Jahnig, F. (1986) *Biophys. J. 50*, 573−582.
38. Beschiaschvili, G., and Seelig, J. (1990) *Biochemistry 29*, 52−58.
39. Schwarz, G., Zong, R. T., and Popescu, T. (1992) *Biochim. Biophys. Acta 1110*, 97−104.
40. Pawlak, M., Meseth, U., Dhanapal, B., Mutter, M., and Vogel, H. (1994) *Protein Sci. 3*, 1788−1805.
41. Marsh, D. (1996) *Biochem. J. 315*, 345−361.
42. Sessions, R. B., Gibbs, N., and Dempsey, C. E. (1998) *Biophys. J. 74*, 138−152.
43. Rex, S., and Schwarz, G. (1998) *Biochemistry 37*, 2336−2345.
44. Ladokhin, A. S., and White, S. H. (2001) *Biochim. Biophys. Acta 1514*, 253−260.
45. Matsuzaki, K., Harada, M., Handa, T., Funakoshi, S., Fujii, N., Yajima, H., and Miyajima, K. (1989) *Biochim. Biophys. Acta 981*, 130−134.
46. Bechinger, B., Kim, Y., Chirlian, L. E., Gesell, J., Neumann, J. M., Montal, M., Tomich, J., Zasloff, M., and Opella, S. J. (1991) *J. Biomol. NMR 1*, 167−173.
47. Oren, Z., and Shai, Y. (1997) *Biochemistry 36*, 1826−1835.
48. Ladokhin, A. S., and White, S. H. (1999) *J. Mol. Biol. 285*, 1363−1369.
49. Merrifield, R. B., Vizioli, L. D., and Boman, H. G. (1982) *Biochemistry 21*, 5020−5031.
50. Gazit, E., Lee, W. J., Brey, P. T., and Shai, Y. (1994) *Biochemistry 33*, 10681−10692.
51. Morton, T. A., Myszka, D. G., and Chaiken, I. M. (1995) *Anal. Biochem. 227*, 176−185.
52. Matsuzaki, K., Murase, O., Fujii, N., and Miyajima, K. (1995) *Biochemistry 34*, 6521−6526.
53. Ladokhin, A. S., Selsted, M. E., and White, S. H. (1997) *Biophys. J. 72*, 1762−1766.
54. Vogel, H. (1987) *Biochemistry 26*, 4562−4572.
55. Shai, Y., and Oren, Z. (2001) *Peptides 22*, 1629−1641.
56. Avrahami, D., Oren, Z., and Shai, Y. (2001) *Biochemistry 40*, 12591−12603.
57. Avrahami, D., and Shai, Y. (2002) *Biochemistry 41*, 2254−2263.
58. Pouny, Y., and Shai, Y. (1992) *Biochemistry 31*, 9482−9490.
59. Oren, Z., and Shai, Y. (1998) *Biopolymers 47*, 451−463.

BI0267846